Key Engineering Materials
ISSN: 1662-9795, Vol. 1049, pp 65-74
doi:10.4028/p-po3dGG

Submitted: 2026-01-19
Revised: 2026-03-02
Accepted: 2026-03-02
Online: 2026-04-15

AI-Driven Design and Optimization of Bending Processes

Diogo Fernandes[1,a], Tomás Parreira[1,b], Daniel Cruz[2,c], Armando Marques[1,d], Pedro Prates[1,3,e], Marta Oliveira[1,f], Abel Santos[2,g], Diogo Neto[1,h] and André Pereira[1,i*]

[1]Centre for Mechanical Engineering, Materials and Processes (CEMMPRE), University of Coimbra, Portugal

[2]Institute of Science and Innovation in Mechanical and Industrial Engineering Department (INEGI), Porto, Portugal

[3]Centre for Mechanical Technology and Automation (TEMA), University of Aveiro, Portugal

[a]diogofer36@gmail.com, [b]tomas.parreira@dem.uc.pt, [c]dcruz@inegi.up.pt, [d]armando.marques@uc.pt, [e]prates@ua.pt, [f]marta.oliveira@dem.uc.pt, [g]abel@fe.up.pt, [h]diogo.neto@dem.uc.pt, [i*]andre.pereira@uc.pt

*corresponding author

Keywords: machine learning, optimization, forming processes, bending.

Abstract. Air bending is a critical operation in the metalworking industry, where dimensional accuracy and process efficiency are essential to ensure product quality and economic viability. This work proposes an AI-driven design and optimization strategy which couples artificial intelligence, specifically artificial neural networks, with a quasi-random search algorithm for the metamodeling and optimization of the air bending process. An extensive simulation database was generated by varying geometrical, material, and process parameters, and neural-network-based metamodels were trained to predict the maximum punch force, maximum thickness reduction, and final bending angle, achieving high predictive accuracy with R^2 values exceeding 0.96. The metamodel was subsequently used to optimize process configurations by simultaneously minimizing the maximum punch force and the maximum thickness reduction while ensuring the target bending angle, leading on average to reductions of 46.7% in maximum force and 31.5% in thickness reduction compared to non-optimized cases. The results demonstrate that artificial intelligence provides an efficient and effective tool for the design and optimization of the bending process, significantly accelerating parameter selection while improving process quality and reducing manufacturing costs.

Introduction

Bending is a widely used sheet metal forming process in the automotive, aerospace, and metalworking industries. Finite Element Analysis is a well-established tool for the development and optimization of bending operations. However, its application (i.e. build of the numerical models, run of the simulations and results analysis) is generally associated with high time costs [1,2], especially when interactive process parameter optimization or robust analysis is required [3]. Furthermore, its high software licensing costs and the need for skilled personnel limit its adoption by small companies [1]. As a result, many of them still rely on traditional trial-and-error approaches, heuristic rules, standards and equations [4–6]. Despite their simplicity, these approaches are associated with inaccuracy and low flexibility due to the assumed simplifications [1,7], such as ignoring the material anisotropy and hardening [4,5].

In the last decade, the increasing availability of big data and computer performance, has encouraged the use of machine learning (ML) techniques to predict the springback and other factors that limit the bending formability (e.g. excessive thinning) [2,8–10]. The application of these techniques requires several numerical simulations of the bending process with different configurations to train the metamodels. The ML approaches should allow the design and optimization of the bending operation without the time costs associated with FEA (i.e., after training the metamodels) and the errors associated with the simplification made in traditional approaches.

However, these approaches still face several challenges, including limited adaptability to new materials and design, simplified material modeling, and reliance on specialized expertise for implementation. These simplifications affect the results quality and limit the flexibility, to adapt to new materials or bending designs, without the expensive cost of training new metamodels. In this sense, its application requires operators with specific knowledge of FEA, ML and optimization techniques. This has limited the application of ML approaches to research studies, hampering the industrial application [11].

With the goal of overcoming the current limitation of ML approaches, in this work is proposed an AI-driven design and optimization strategy capable of adapting to new materials or bending designs. For such, artificial neural networks (ANNs) are employed for the metamodeling and optimization of an air bending process. The numerical model of the bending operation was first parameterized to automatically adapt to different bending configurations (e.g., punch and die geometries). Using a database generated from multiple numerical simulations, ANNs were trained to develop a metamodel capable of predicting various process outputs, namely the final bending angle, maximum thickness reduction, and maximum punch force. Once the metamodel was established, a quasi-random search optimization based on a Sobol sequence was used to optimize the process configuration with the goal of simultaneously minimizing the maximum applied force and thickness reduction, while ensuring that the final bending angle remained within the desired tolerances.

Air Bending

Sheet metal bending is a fundamental metal forming operation used to manufacture components across a wide range of industrial sectors. The process is based on the controlled displacement of a punch that induces plastic deformation in a metal sheet [12]. Among the available bending techniques, air bending is one of the most widely adopted due to its flexibility and efficiency. In air bending, the blank is supported by the die at two contact points, and full punch–die conformity is not required. This characteristic reduces tooling specificity, increases process flexibility, and limits excessive forming loads, making the process suitable for a wide range of part geometries and bending angles [13]. After forming the blank, the punch is removed and the elastic recovery occurs (springback) which causes deviations from the target bend angle and typically requires compensation strategies to ensure dimensional accuracy [14,15].

The air bending process is governed by the interaction of geometric, process, and material parameters. Fig. 1 illustrates the main geometric parameters associated with the punch, die, and blank, including the punch radius, R_p, the punch opening angle, β, the upper die radius, R_s, the die opening angle, γ, the die length, V, and the blank width, W, length, L, and thickness, t_0. In addition to these geometric parameters, the operator can adjust the process parameters, namely the bending direction, θ relatively to the rolling direction (RD), the lubrication conditions (represented by the friction coefficient, μ_0) and the punch relative displacement, ΔP. In this work, ΔP is defined as a normalized punch stroke, where ΔP = 100% corresponds to the punch reaching the bottom of the die. Additionally, the punch opening angle is assumed to match the die opening angle, as it has no effect on the air bending process because contact occurs only at the punch tip. Material parameters describing hardening behavior and anisotropy are addressed in the following section.

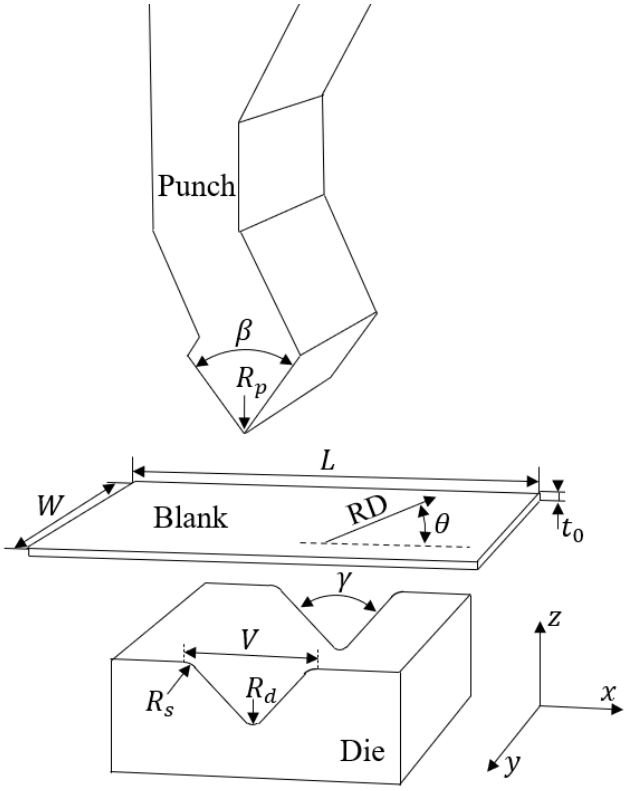

Fig. 1. Geometrical parameters in the air bending process.

Numerical Model

The mechanical behaviour of the material under study is assumed to be: isotropic elastic, described by the generalised Hooke's law, which has two parameters, the Young's modulus, E, and the Poisson's ratio, v; and orthotropic plastic, described by the Swift hardening law [16] and the Hill'48 [17] yield criterion. This yield criterion is defined by:

$$F(\sigma_{yy}-\sigma_{zz})^2+G(\sigma_{zz}-\sigma_{xx})^2+H(\sigma_{xx}-\sigma_{yy})^2+2L\tau_{yz}^2+2M\tau_{xz}^2+2N\tau_{xy}^2=Y^2, \quad (1)$$

where σ_{xx}, σ_{yy}, σ_{zz}, τ_{xy}, τ_{yz} and τ_{xz} are the components of the Cauchy stress tensor; Y is the yield stress; F, G, H, L, M and N are the Hill'48 anisotropy parameters. These parameters follow the conditions $G+H=1$ and $L = M = 1.5$ (von Mises). The Swift hardening law is defined by:

$$Y=C\,(\varepsilon_0+\bar{\varepsilon}^p)^n, \quad (2)$$

where $\bar{\varepsilon}^p$ is the equivalent plastic strain and C, ε_0 and n are the hardening constants. The initial yield stress is given by $Y_0=C\varepsilon_0^n$.

The friction between the tools and the blank was assumed to be described by Coulomb's law with a constant friction coefficient, μ_0. The contact problem is solved using the augmented Lagrangian method. The blank is discretised with 30576 (8-node hexahedral solid) elements, with 6 elements in thickness, combined with a selective reduced integration technique [18]. The tools are modelled as rigid bodies and described by Bezier surfaces; their displacement is restricted with exception of the punch which is allowed to move on the vertical direction (z-axis in Fig. 1). The numerical simulations were performed using the software DD3IMP (Deep Drawing 3D Implicit Code) [18], which uses an updated Lagrangian scheme to integrate the constitutive law in an implicit way. Each simulation took an average of about 1 hour to complete on computers equipped with an Intel® Core™ i7-6850K (4.0 GHz).

AI-Driven Design Strategy

In this section, the strategy for optimizing air bending process parameters is presented. First, artificial neural networks are used to train metamodels capable of predicting three process outputs (namely, the final bending angle, the maximum thickness reduction, and the maximum punch force) based on the material and geometric configuration. Second, an optimization procedure is applied to modify the process parameters within the metamodel, aiming to minimize the maximum punch force and thickness reduction while ensuring that the final bending angles remain within the required tolerances.

Metamodeling.

The metamodels were built based on a database consisting of 3 bending results (outputs) and 15 process and material parameters (inputs). As previously mentioned, the three outputs are the maximum punch force during the bending, F_{max}, the final bending angle of the component, α, (as represented in Fig. 2) and the maximum thickness reduction along the bending line, Δt_{max}, given by:

$$\Delta t_{max}\ [\%] = \frac{t_0 - t_{min}}{t_0} \times 100, \tag{3}$$

where t_0 is the initial blank thickness and t_{min} is the minimal thickness along the bending line, represented in Fig. 2.

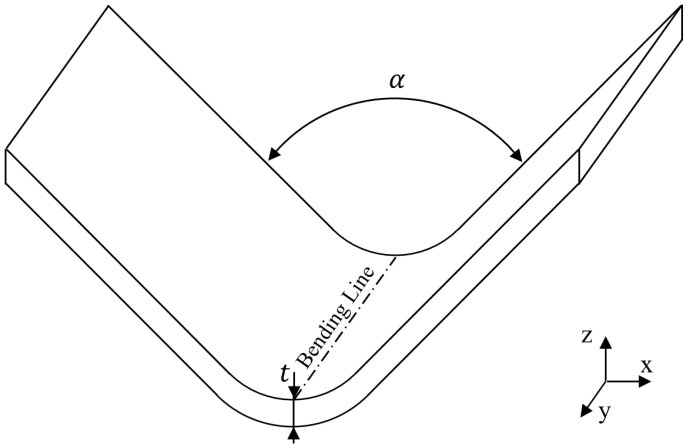

Fig. 2. Representation of the final bending angle, α, and the bending line where the minimal thickness is evaluated.

A total of 15 input parameters were considered, comprising material, geometrical, and process parameters. The material parameters include the anisotropy coefficients according to Hill's yield criterion, r_0, r_{45}, r_{90}, as well as the parameters of Swift's hardening law, Y_0, C and n. The geometrical parameters comprise the blank width, W, and initial thickness, t_0, the punch radius, R_p, the upper die radius, R_s, the die length, V, and the die opening angle, γ. The process parameters are the lubrication conditions represented by the friction coefficient, μ_0, the normalized punch displacement, ΔP, and the bending direction, θ, defined as the angle between the sheet rolling direction and the axis perpendicular to the bending line (x-axis in Fig. 1). Some of these parameters are illustrated in Fig. 1.

To build the database, the bending results were gathered from 2000 numerical simulations of the air bending process, each one representing a distinct material and process configuration. A Sobol sequence [19] was employed to generate the 2000 samples, ensuring a uniform coverage of the 15th dimensional input space, whose parameters range are given in Table 1. The maximum punch force and maximum thickness reduction outputs were first log-scaled to mitigate the influence of outliers. Due to the different orders of magnitude among the parameters, all data were subsequently min–max normalized to the range [0, 1]. For testing and training the metamodel, the database was divided into two independent subgroups. A total of 1600 simulations (80%) were used for training and calibration

of the metamodel, while the remaining 400 simulations (20%) were reserved for testing and used exclusively to assess the predictive accuracy and generalization capability of the trained metamodel.

Table 1. Minimum and maximum values of the 15 input parameters.

	r_0	r_{45}	r_{90}	Y_0	C	n	t_0	W	γ	V	R_s	R_p	μ_0	θ	ΔP
	[-]	[-]	[-]	[MPa]	[MPa]	[-]	[mm]	[mm]	[º]	[mm]	[mm]	[mm]	[-]	[º]	[%]
Max	3	3	3	1000	700	0.3	3	100	120	60	5	3	0.2	90	80
Min	0.5	0.5	0.5	100	100	0.05	0.5	10	60	20	1	1	0.05	0	20

The metamodel was developed using an artificial neural network (ANN) implemented with the TensorFlow/Keras library. A sequential architecture was adopted, comprising an input layer with 15 neurons, corresponding to the input variables, followed by five hidden layers with 700, 400, 500, 700, and 300 neurons, respectively. The output layer consisted of three neurons, representing the target outputs. All hidden layers employed the Rectified Linear Unit (ReLU) activation function. The network was trained using the Adaptive Moment Estimation (ADAM) optimizer with a learning rate of 0.0018, and a dropout rate of 0.2 was applied to mitigate overfitting.

The predictive performance of the metamodels was evaluated for the 400 test samples. Fig. 3 shows a comparison between the real and predicted values of the bending results. To quantify the predictive performance, Table 2 presents the Mean Absolute Error (MAE), Root Mean Squared Error (RMSE), and the coefficient of determination (R^2) obtained for the three outputs. As seen, the predicted values are generally similar to the real values, which can be confirmed by the relatively high R^2 values (above 0.96) and the relatively low MAE and RMSE metrics. It can be concluded that the bending angle and the maximum punch force can be accurately predicted, slightly worst predictions are obtained for the maximum thickness reduction.

Table 2. Mean Absolute Error (MAE), Root Mean Squared Error (RMSE), and the coefficient of determination (R^2) evaluated for each output.

	α	F_{max}	Δt_{max}
MAE	1.29°	425 N	0.25%
RMSE	1.69°	815 N	0.41%
R^2	0.99	0.99	0.96

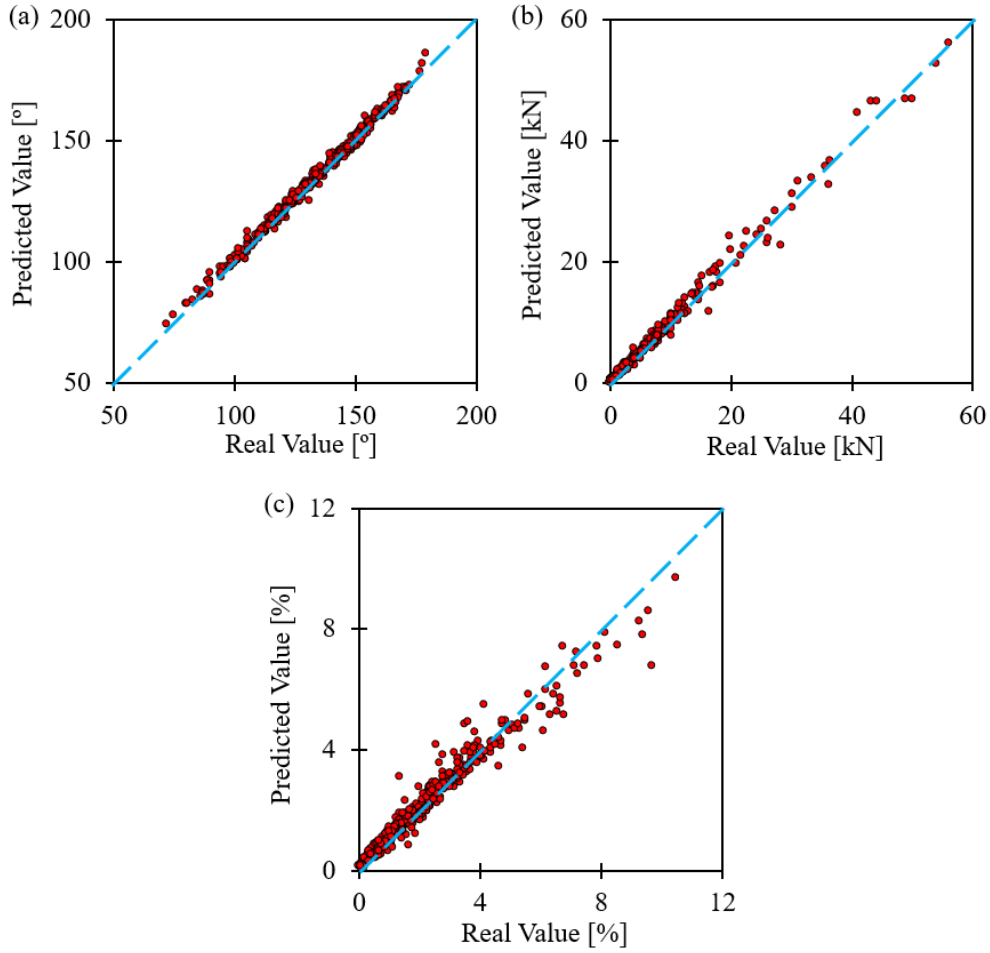

Fig. 3. Predicted (metamodel) and real values of the bending results: (a) Final bending angle, α; (b) Maximum punch force, F_{max}; (c) Maximum thickness reduction, Δt_{max}.

Process Optimization.

The metamodel was used to determine the optimal process parameters required to achieve the desired bending results, enabling its use as a decision-support tool in an industrial context. To this end, an optimization strategy was employed to identify the process and geometrical parameters (μ_0, ΔP, R_p, R_s, V and γ). A Quasi-Random Search optimization strategy based on a Sobol sequence was adopted to explore the parameter space efficiently and uniformly, while maintaining low computational cost through the use of the metamodel for predictions. The material parameters (r_0, r_{45}, r_{90}, Y_0, C and n), blank dimensions (W and t_0) and the bending direction (θ), typically known a priori by the operator, were kept constant. In contrast, the process and geometrical parameters (μ_0, ΔP, R_p, R_s, V and γ), which must be optimized, were systematically varied accordingly with the Sobol sequence. A total of 50000 distinct process configurations were generated, each evaluated using the metamodel to predict the corresponding outputs (α, F_{max} and Δt_{max}). The next step consisted in selecting the process configuration with a final bending angle, α, within a predefined tolerance of the target value. In this work, the tolerance was set to 0.0005º, although it can be adjusted by the operator according to part requirements.

After identifying the viable subset of process configurations (i.e., those that achieve the bending angle required by the operator), a secondary analysis was conducted on two critical performance metrics: the maximum bending force and the maximum thickness reduction. The objective is to select the process configuration that requires lower bending forces, thereby improving process efficiency, while simultaneously minimizing the maximum thickness reduction, preserving part quality. To this end, an objective function, ψ, was defined as:

$$\psi = F^*_{max} + \Delta t^*_{max}, \tag{4}$$

where F^*_{max} and Δt^*_{max} are the normalized maximum punch force and maximum thickness reduction, obtained via min–max normalization. The optimal solution is the configuration in the viable subset that minimizes ψ.

Results

The AI-driven design strategy was applicated for 10 different cases, in which the material parameters (r_0, r_{45}, r_{90}, Y_0, C and n), blank dimensions (W and t_0) and the bending direction (θ) were assumed to be known, as summarized in Table 3. For the remaining input parameters (μ_0, ΔP, R_p, R_s, V and γ), a set of 50000 distinct bending configurations was generated, aiming to preserve the target final bending angle (α) indicated in Table 4 (original configuration), while simultaneously minimizing the maximum force (F_{max}) and the maximum thickness reduction (Δt_{max}). Table 4 presents both the original (non-optimized parameters) and the AI-design configurations. The grey columns show the numerical bending results obtained for each configuration.

Table 3. Known material and process parameters for the 10 cases.

Case	r_0 [-]	r_{45} [-]	r_{90} [-]	Y_0 [MPa]	C [MPa]	n [-]	t_0 [mm]	W [mm]	θ [º]
1	0.92	2.36	1.19	543	1094	0.19	1.78	85	2
2	2.80	2.98	1.81	318	1243	0.26	1.10	16	30
3	1.55	1.73	0.56	768	1287	0.13	2.45	62	85
4	1.24	2.67	2.75	205	479	0.22	0.76	74	98
5	2.49	1.42	1.50	655	1054	0.10	2.11	28	43
6	0.61	0.80	2.13	880	1726	0.16	1.44	97	16
7	1.86	2.05	0.88	430	2958	0.29	2.79	51	71
8	2.02	1.27	1.35	261	318	0.05	0.59	91	78
9	0.77	2.52	2.60	711	1605	0.18	1.94	45	23
10	2.64	1.89	0.72	936	2474	0.24	1.27	68	5

Table 4. Original and AI-designed process configurations, along with their numerical bending results.

	Original Configuration									AI-Design Configuration								
Case	γ [º]	V [mm]	R_s [mm]	R_p [mm]	μ_0 [-]	ΔP [%]	Δt_{max} [%]	F_{max} [N]	α [º]	γ [º]	V [mm]	R_s [mm]	R_p [mm]	μ_0 [-]	ΔP [%]	Δt_{max} [%]	F_{max} [N]	α [º]
1	115	30	3.3	1.1	0.11	20.6	1.02	7044	168.9	113	59	3.4	2.3	0.06	21.4	0.42	3351	170.0
2	68	20	2.2	1.6	0.06	35.6	3.05	856	130.6	96	60	2.2	1.8	0.22	56.8	1.68	200	128.6
3	99	41	4.3	2.6	0.16	65.6	2.28	8078	126.4	109	59	3.3	1.3	0.05	74.4	1.95	5024	127.3
4	107	25	2.7	2.3	0.13	73.1	1.09	735	126.8	68	61	3.6	2.4	0.21	40.6	0.70	268	126.1
5	76	46	4.8	1.3	0.23	43.1	4.11	3056	130.0	60	58	4.7	1.7	0.22	34.2	3.57	2309	128.6
6	92	57	1.7	1.8	0.18	28.1	0.43	4388	161.9	116	61	2.9	1.4	0.24	42.0	0.35	4123	163.1
7	61	36	3.8	2.9	0.08	58.1	4.66	16400	94.9	79	59	2.6	1.6	0.08	72.5	3.21	7715	94.4
8	80	44	3.0	2.2	0.10	24.3	0.63	249	156.2	74	61	4.3	1.5	0.15	25.3	0.54	181	153.0
9	111	23	5.1	1.2	0.20	54.3	2.86	12325	143.8	109	59	1.2	2.2	0.19	55.6	1.42	3250	143.4
10	64	33	2.0	1.7	0.25	69.3	1.98	5297	96.3	65	60	3.5	1.2	0.13	77.8	1.31	2509	96.9

From Table 4, it is evident that the AI-Design strategy exhibits a clear and systematic tendency toward larger die lengths (V), with all optimized cases converging to the maximum allowable value of 60 mm. This indicates that AI-Design strategy consistently drives the die length to the upper bound of the design space to minimize the maximum punch force, in agreement with the inverse relationship between die length and punch force. From a theoretical perspective, the friction coefficient would be expected to converge to its lowest possible value to further reduce the punch force. However, no

consistent trend is observed in the optimized configurations, suggesting that friction has a comparatively minor influence on the air bending process. The remaining parameters do not exhibit consistent trends but are adjusted case by case, compensating the increase in the die length, in order to achieve the optimization objectives.

Regarding the bending results, Fig. 4 (a) illustrates the close agreement between the final bending angles obtained from numerical simulations using the original and AI-Design configurations for the 10 cases, with an average relative difference of 0.87%. Fig 4 (b) and (c) highlight the substantial reductions achieved through the AI-Design, with average relative decreases of 31.5% in the maximum thickness reduction and 46.7% in the maximum punch force.

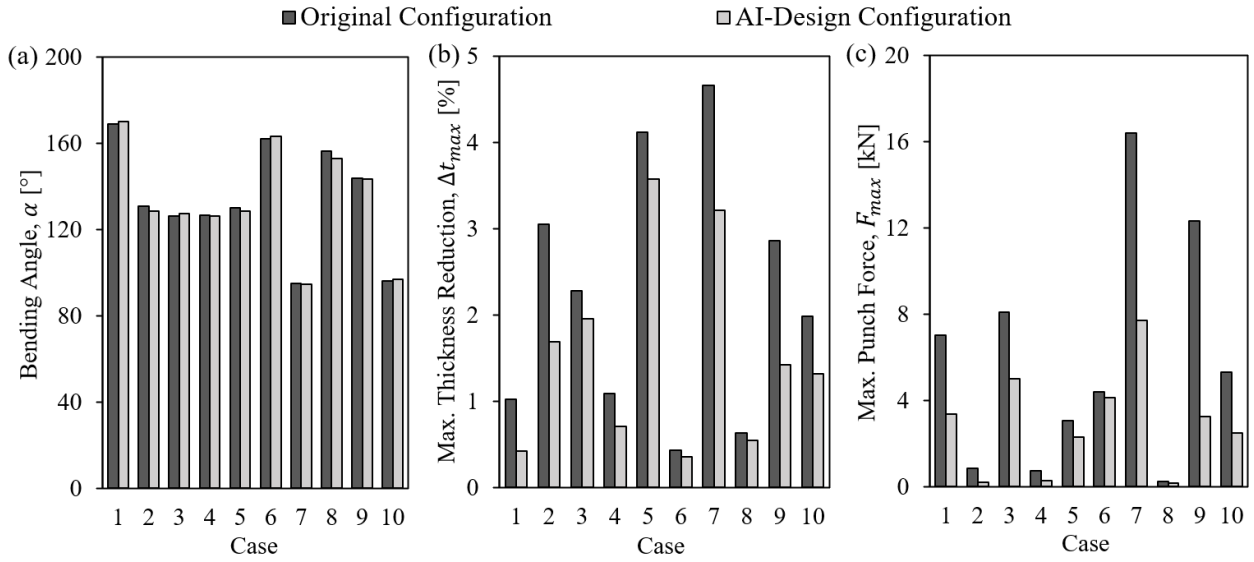

Fig. 4. Bending results obtained from the numerical simulation of the air bending process, using the original and AI-Design configuration: (a) final bending angle, α; (b) maximum thickness reduction, Δt_{max}; (c) maximum punch force, F_{max}.

It should be noted that the parameters to be optimized were assumed to be continuous. In practice, however, there is a limited choice in the possible die and punch geometries that are available. Nevertheless, the used Quasi-Random Search optimization strategy can still be applied to mixed discrete–continuous problems, simply by respecting the discrete options for certain parameters during the generation of the process configurations.

Conclusion

This work investigated the application of artificial intelligence techniques for the metamodeling and optimization of the air bending process. An extensive numerical database was created by varying geometrical, material, and operational parameters, covering a wide range of process configurations. Based on this dataset, a neural-network based metamodel was trained to predict three process results: the maximum punch force, the maximum thickness reduction and the final bending angle. The metamodel demonstrated strong predictive performance, with R^2 values exceeding 0.96 for all outputs and low prediction errors (RMSE and MAPE).

During optimization, the metamodel enabled the identification of process configurations that simultaneously minimize the maximum punch force and thickness reduction while ensuring the target final bending angle. On average, the optimized configurations achieved the same bending angle with average relative decreases of 46.7% in the maximum force and 31.5% in the maximum thickness reduction compared to the non-optimized configurations. This optimization, which would be computationally intensive using numerical simulations alone, was highly efficient due to the metamodel application.

Overall, the results confirm that integrating artificial intelligence provides a powerful tool for metal forming process design, significantly accelerating the design and parameter optimization stages

while improving process quality and reducing manufacturing costs. Future work will focus on industrial validation of the optimized solutions, extending the methodology to multi-stage bending operations, optimizing additional performance metrics such as dimensional accuracy, and exploring more advanced AI algorithms to further enhance the generalization capability of the design strategy.

Acknowledgment

This work is sponsored by national funds through FCT – Fundação para a Ciência e a Tecnologia, under the project UID/00285-Centre for Mechanical Engineering, Materials and Processes and LA/P/0112/2020. It was also supported by the projects RealForm (ref. 2022.02370.PTDC), SmartBending (ref. 2023.14606.PEX), LSD-TRIP (ref. COMPETE2030-FEDER-00778700) and A3Shell (ref. COMPETE2030-FEDER-02233400) The author Tomás Parreira was supported by doctoral grant from FCT (2024.00961.BD). All support is gratefully acknowledged.

References

[1] J. Ma, T. Welo, Analytical Springback Assessment in Flexible Stretch Bending of Complex Shapes, *Int. J. Mach. Tools Manuf.*, 160 (2021) 103653, doi:10.1016/j.ijmachtools.2020.103653.

[2] A.E. Marques, P.A. Prates, A.F.G. Pereira, M.C. Oliveira, J.V. Fernandes, B.M. Ribeiro, Performance Comparison of Parametric and Non-Parametric Regression Models for Uncertainty Analysis of Sheet Metal Forming Processes, *Metals (Basel)*, 10 (2020) 457, doi:10.3390/met10040457.

[3] J.H. Wiebenga, A.H. van den Boogaard, G. Klaseboer, Sequential Robust Optimization of a V-Bending Process Using Numerical Simulations, *Struct. Multidiscip. Optim.*, 46 (2012) 137–153, doi:10.1007/s00158-012-0761-0.

[4] S.A. Hindman, M.J. Bussey, Custom Equations for the Unfolding of Sheet Metal, Patent US8131516 B2 (2012).

[5] DIN 6935, Cold Bending of Flat Rolled Steel (2011), doi:10.31030/1813521.

[6] M.R. Jamli, N.M. Farid, The Sustainability of Neural Network Applications within Finite Element Analysis in Sheet Metal Forming: A Review, *Measurement*, 138 (2019) 446–460, doi:10.1016/j.measurement.2019.02.034.

[7] S.S. Miranda, M.R. Barbosa, A.D. Santos, J.B. Pacheco, R.L. Amaral, Forming and Springback Prediction in Press Brake Air Bending Combining Finite Element Analysis and Neural Networks, *J. Strain Anal. Eng. Des.*, 53 (2018) 584–601, doi:10.1177/0309324718798222.

[8] D.J. Cruz, M.R. Barbosa, A.D. Santos, R.L. Amaral, J.C. de Sa, J.V. Fernandes, Recurrent Neural Networks and Three-Point Bending Test on the Identification of Material Hardening Parameters, *Metals (Basel)*, 14 (2024) 84, doi:10.3390/met14010084.

[9] D.A. Molitor, V. Arne, C. Kubik, G. Noemark, P. Groche, Inline Closed-Loop Control of Bending Angles with Machine Learning Supported Springback Compensation, *Int. J. Mater. Form.*, 17 (2024) 8, doi:10.1007/s12289-023-01802-y.

[10] W. Muhammad, R. Mahmoud, F. Anis, U.R.B. Saad, Prediction of Springback Using the Machine Learning Technique in High-Tensile Strength Sheet Metal during the V-Bending Process, *Jordan J. Mech. Ind. Eng.*, 17 (2023) 481–488, doi:10.59038/jjmie/170403.

[11] M.A. Dib, B. Ribeiro, P. Prates, Federated Learning as a Privacy-Providing Machine Learning for Defect Predictions in Smart Manufacturing, *Smart Sustain. Manuf. Syst.*, 5 (2021) 1–17, doi:10.1520/SSMS20200029.

[12] D. Wang, Y. Xu, B. Duan, Y. Wang, M. Song, H. Yu, H. Liu, Intelligent Recognition Model of Hot Rolling Strip Edge Defects Based on Deep Learning, *Metals (Basel)*, 11 (2021) 223, doi:10.3390/met11020223.

[13] D. Fei, P. Hodgson, Experimental and Numerical Studies of Springback in Air V-Bending Process for Cold Rolled TRIP Steels, *Nucl. Eng. Des.*, 236 (2006) 1847–1851, doi:10.1016/j.nucengdes.2006.01.016.

[14] X. Li, Effects of Air Bending Parameters on Springback Using Finite Element Analysis, *Appl. Mech. Mater.*, 423–426 (2013) 978–983, doi:10.4028/www.scientific.net/AMM.423-426.978.

[15] M.S. Buang, S.A. Abdullah, J. Saedon, Effect of Die and Punch Radius on Springback of Stainless Steel Sheet Metal in the Air V-Die Bending Process, *J. Mech. Eng. Sci.*, 8 (2015) 1322–1331, doi:10.15282/jmes.8.2015.7.0129.

[16] H.W. Swift, Plastic Instability under Plane Stress, *J. Mech. Phys. Solids*, 1 (1952) 1–18, doi:10.1016/0022-5096(52)90002-1.

[17] R. Hill, A Theory of the Yielding and Plastic Flow of Anisotropic Metals, *Proc. R. Soc. A Math. Phys. Eng. Sci.*, 193 (1948) 281–297, doi:10.1098/rspa.1948.0045.

[18] L.F. Menezes, C. Teodosiu, Three-Dimensional Numerical Simulation of the Deep-Drawing Process Using Solid Finite Elements, *J. Mater. Process. Technol.*, 97 (2000) 100–106, doi:10.1016/S0924-0136(99)00345-3.

[19] I.M. Sobol', On the Distribution of Points in a Cube and the Approximate Evaluation of Integrals, *USSR Comput. Math. Math. Phys.*, 7 (1967) 86–112, doi:10.1016/0041-5553(67)90144-9.